

Critical behavior in spin-reorientation phase transitions: ($\text{Er}_x\text{R}_{1-x}$) $_2\text{Fe}_{14}\text{B}$ ($R = \text{Nd}, \text{Dy}$) magnets

A. del Moral, M. R. Ibarra, C. Marquina, J. I. Arnaudas, and P. A. Algarabel

*Laboratorio de Magnetismo de Sólidos, Departamento Física de la Materia Condensada
and Instituto de Ciencia de Materiales de Aragón, Facultad de Ciencias,*

Consejo Superior de Investigaciones Científicas, Universidad de Zaragoza, E-50009 Zaragoza, Spain

(Received 4 October 1988; revised manuscript received 15 March 1989)

The critical behavior of spin-reorientation phase transitions in the hard magnetic intermetallics ($\text{Er}_x\text{R}_{1-x}$) $_2\text{Fe}_{14}\text{B}$ ($R = \text{Dy}$ and Nd) has been studied with ac low-field susceptibility, χ_H , and cone-angle measurements. A simple model for scaling the low-field susceptibility has been developed and applied to the present series of compounds. The critical exponents for χ_H have been determined for some well-behaved compounds.

I. INTRODUCTION

The attention paid to critical behavior in spin-reorientation (SR) phase transitions is scarce.¹ In such a transition the average magnetization rotates from an initial easy direction towards a final one; in many situations the reorientation angle is $\pi/2$, but in other cases the reorientation is incomplete.^{2,3} We present here one of the first observations,^{4,5} to our knowledge, of critical behavior in SR phase transitions, based on ac initial susceptibility measurements [see Figs. 1(a)–1(d)] done on the hard magnetic pseudoternaries ($\text{Er}_x\text{R}_{1-x}$) $_2\text{Fe}_{14}\text{B}$ with $R = \text{Nd}$ and Dy , which are also systems of great technological import.⁶ These systems crystallize in the tetragonal structure (space group $P4_2/mnm$)⁶ and are ferromagnetically (or ferrimagnetically for the heavy R) ordered below $T_c = 585$ K ($\text{Dy}_2\text{Fe}_{14}\text{B}$), $T_c = 580$ K ($\text{Nd}_2\text{Fe}_{14}\text{B}$), and $T_c = 550$ K ($\text{Er}_2\text{Fe}_{14}\text{B}$).⁷ For temperatures $T > T_{\text{SR1}}$, where T_{SR1} is the temperature at which the SR transition starts, the magnetization lies on an easy direction along the c axis; for $T < T_{\text{SR1}}$, the magnetic structure is either conical or planar (see Fig. 2), along the easy basal plane of the tetragonal structure.⁸

Although the detailed magnetic phase diagrams of such pseudoternaries have been treated with more detail elsewhere,^{9–12} we will discuss here those features specifically related to the critical behavior observed at the SR phase transitions in those materials. In the present series of pseudoternaries it is important to distinguish between those suffering only a SR at T_{SR1} [that is the case of ($\text{Er}_x\text{Dy}_{1-x}$) $_2\text{Fe}_{14}\text{B}$; see Figs. 1(a) and 2(a)] and those undergoing two transitions at temperatures T_{SR1} and T_{SR2} [the case of ($\text{Er}_x\text{Nd}_{1-x}$) $_2\text{Fe}_{14}\text{B}$ compounds, for $0.2 \leq x \leq 0.6$; see Figs. 1(b)–1(d) and 2(b)].⁹ In more detail, $\text{Nd}_2\text{Fe}_{14}\text{B}$ is magnetically axial (A) for $T > T_{\text{SR1}}$ ($= 125.9$ K), where it suffers a SR transition [see Fig. 1(b)] to a conical phase never finished (final angle at 0 K, 28°); this transition is believed to be due to the competition of anisotropies between the Nd^{3+} sites (4f and 4g) and the Fe sublattices, which impose an axial symme-

try.¹³ On the other hand $\text{Er}_2\text{Fe}_{14}\text{B}$ undergoes, at $T_{\text{SR1}} = 321.8$ K, a SR transition [see Fig. 1(a)] from axial symmetry to a completely planar (P) one (for $T < T_{\text{SR1}}$). Such a transition is quite sharp, taking place within an interval of ≈ 2 K, and it is believed to be due to the competition between the Fe axial anisotropy and the planar one of the Er^{3+} .

The substitution of Er by Dy in $\text{Er}_2\text{Fe}_{14}\text{B}$ steadily lowers T_{SR1} down to $x = 0.5$, and induces the appearance of a stable conical (C) phase, which evolves further to a planar one for $x > 0.8$. These features have recently been shown by means of measurements of the coning angle [see Fig. 2(a)] and model crystal-field (CEF) calculations.¹¹ However, no anomaly in the initial susceptibility at the $C \rightarrow P$ transition has been detected, probably because it is a continuous evolution and not a proper phase transition. The case of the ($\text{Er}_x\text{Nd}_{1-x}$) $_2\text{Fe}_{14}\text{B}$ series is quite different; the substitution of Nd by Er in $\text{Nd}_2\text{Fe}_{14}\text{B}$ produces the appearance of a planar phase at T_{SR1} for $x > 0.6$ (Ref. 10), the planar anisotropy of Er^{3+} in the CEF being responsible for such a phase. However, for $0.2 \leq x \leq 0.6$, as the measurements of the cone angle also show [see Fig. 2(b)],¹⁰ and the present ac initial susceptibility measurements reflect [see Figs. 1(b)–1(d)], there likely exist two phase transitions: one at T_{SR1} from $A \rightarrow C_1$ (where C_1 is a conical phase) and a second one at T_{SR2} from C_1 to a second conical phase C_2 (order-order transition), where the cone angle becomes well stabilized and therefore the SR in such a system is also incomplete. The complex magnetic phase diagram for this series is fully shown in Fig. 3.

II. MODEL OF SCALING IN SR PHASE TRANSITION

We will now consider the scaling behavior of the initial low-field susceptibility, which is one of the probes available to study the critical behavior of SR transitions,^{4,5} and which has been applied to the present compounds. Therefore we consider that the Gibbs thermodynamic potential is a function $G = G(T, H, \theta)$, where T and H , re-

spectively, are the temperature and internal magnetic field in the system, and θ is the average SR angle, measured from the c axis. The field susceptibility can be written as

$$\chi_H = \left[\frac{\partial^2 G}{\partial H^2} \right]_T, \quad (1)$$

which can also be developed as

$$\chi_H = \left[\frac{\partial^2 G}{\partial H \partial \theta} \right]_T \left[\frac{\partial \theta}{\partial H} \right]_T + \left[\frac{\partial G}{\partial \theta} \right]_{T,H} \left[\frac{\partial^2 \theta}{\partial H^2} \right]_T. \quad (2)$$

If we admit that we are relatively far enough from T_{SR1} so that the critical fluctuations of θ are weak enough to apply equilibrium thermodynamics, then $(\partial G / \partial \theta)_{T,H} = 0$. Introducing now the magnetization along the applied field direction given by $M = -(\partial G / \partial H)_{T,\theta}$, Eq. (2) can be transformed to

$$\chi_H = -\chi_\theta \left[\frac{\partial M}{\partial \theta} \right]_{T,H}, \quad (3)$$

where $\chi_\theta = (\partial \theta / \partial H)_T$ is the natural susceptibility in this kind of transition, inasmuch as θ , the SR angle, is the natural order parameter.¹ Considering that the applied magnetic field is along the easy initial c axis, then $M = M_s \cos \theta$, where $M_s = M_s(T)$ is the spontaneous magnetization. Since θ is the order parameter we will restrict ourselves to regions where $T \approx T_{SR1}$ and θ is small. Then from Eq. (3) we immediately obtain

$$\chi_H \approx M_s \theta \chi_\theta = \frac{1}{2} M_s \frac{\partial(\theta^2)}{\partial H}. \quad (4)$$

Now we are able to consider the critical scaling. As usual¹⁴ we will consider two ways of approximation to the origin of the (T, H) plane: $t \rightarrow 0$ for $H = 0$, and $H \rightarrow 0$ for $t = 0$ [t is the reduced temperature, $t = (T - T_{SR1}) / T_{SR1}$].

(i) For $t \rightarrow 0$ (and $H = 0$) the order parameter θ will follow the standard scaling behavior,¹⁴

$$\theta = |t|^{\beta_{SR}} f(H/|t|^{\beta_{SR}\delta_{SR}}), \quad (5)$$

where β_{SR} and δ_{SR} are SR critical exponents for $T < T_{SR1}$

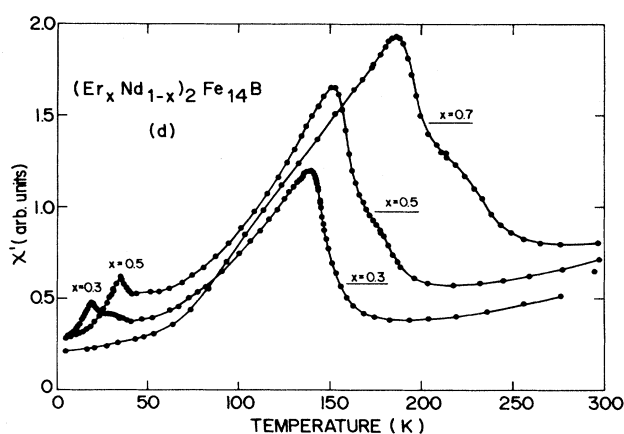
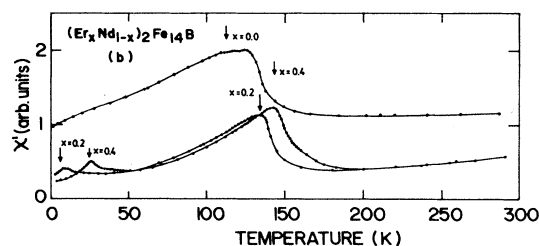
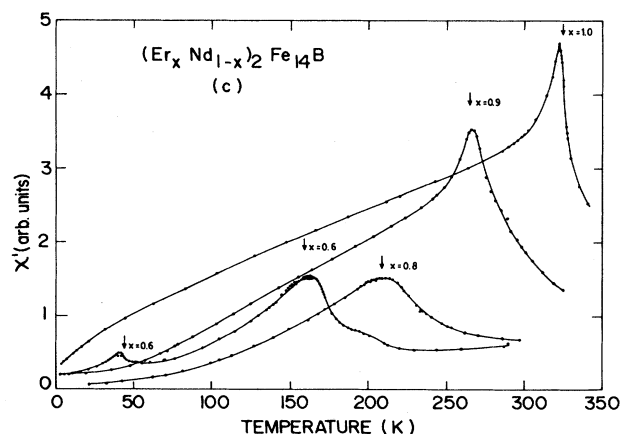
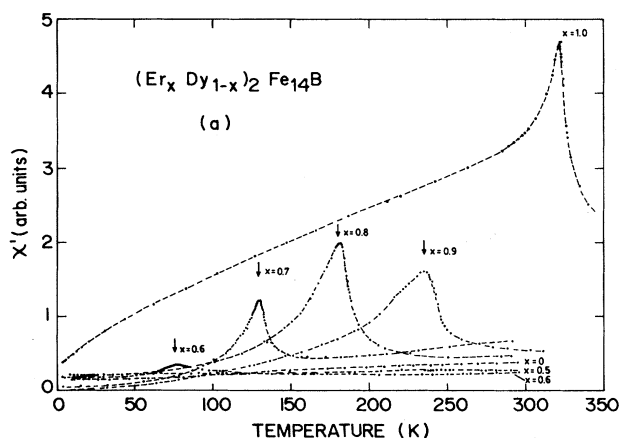


FIG. 1. Thermal variation of the ac (15 Hz) low-field (≈ 30 mOe) magnetic susceptibility (a) for the $(\text{Er}_x \text{Dy}_{1-x})_2 \text{Fe}_{14}\text{B}$ series of intermetallics (the lines are to guide the eye); (b) for the $(\text{Er}_x \text{Nd}_{1-x})_2 \text{Fe}_{14}\text{B}$ series ($0 \leq x \leq 0.4$); (c) for $0.6 \leq x \leq 1$; (d) for $x = 0.3, 0.5$, and 0.7 concentrations.

and f is an arbitrary scaling function of the reduced field $x \equiv H/|t|^{\beta_{SR}\delta_{SR}}$. From Eqs. (4) and (5) and using Widom scaling relation $\beta_{SR}(\delta_{SR}-1)=\gamma'_{SR}$, we immediately obtain

$$\chi_H = M_S |t|^{\beta_{SR}-\gamma'_{SR}} f(x) \dot{f}(x). \quad (6)$$

For a short interval of temperature around T_{SR1} , M_S varies smoothly.^{11,15} Besides, for $x=0$, $f(x)=\text{const}$ and $\dot{f}(x) \equiv df/dx = \text{const}$, and defining the auxiliary exponent $\omega'_{SR} \equiv \gamma'_{SR} - \beta_{SR}$, we finally obtain, for $t < 0$ ($T < T_{SR1}$),

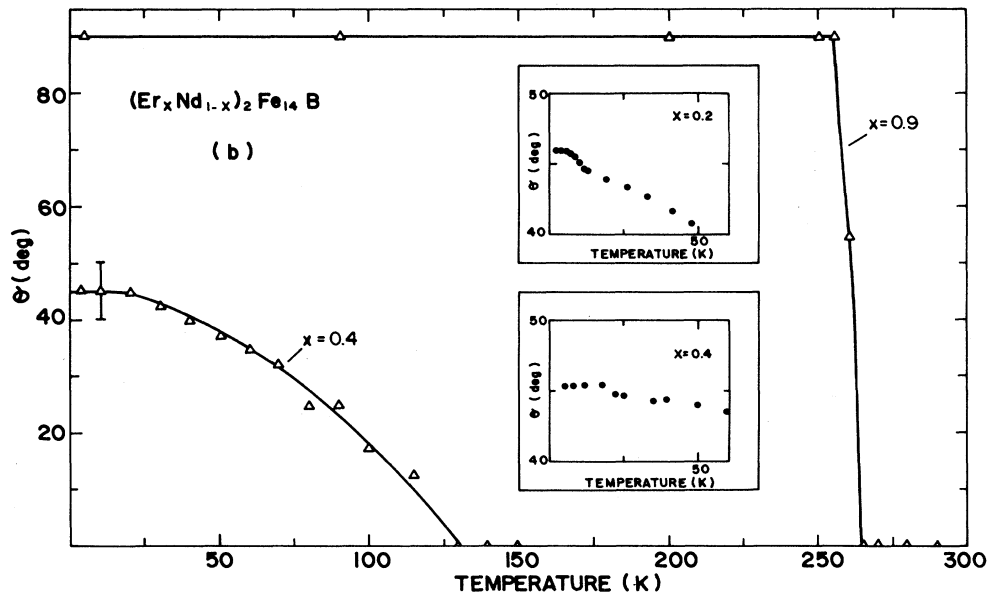
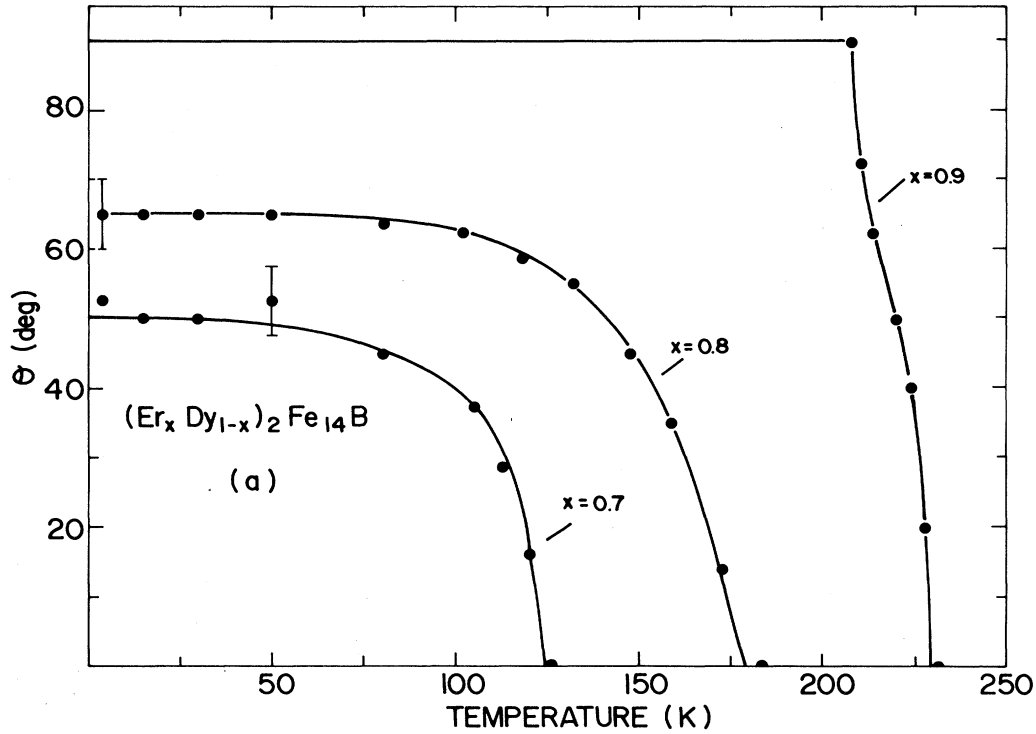


FIG. 2. (a) Thermal variation of the spin-reorientation angle, from the c axis, for some compounds of the $(\text{Er}_x \text{Dy}_{1-x})_2 \text{Fe}_{14}\text{B}$ series, as determined from parallel and perpendicular to the field magnetization measurements (polar plots). The bars indicate the experimental error, and the lines are guides for the eye. (b) The same as for (a) for the $(\text{Er}_x \text{Nd}_{1-x})_2 \text{Fe}_{14}\text{B}$ series. The insets show the SR reorientation angle $\theta = \theta(T_{SR2}) + \phi$ below T_{SR2} , in order to exhibit the weak temperature dependence of the order parameter ϕ .

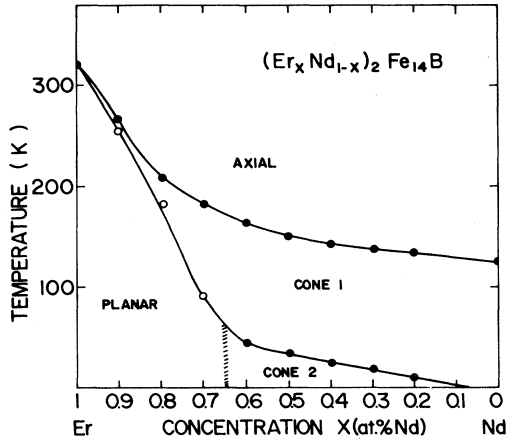


FIG. 3. Magnetic phase diagram for the $(\text{Er}_x\text{Nd}_{1-x})_2\text{Fe}_{14}\text{B}$ series of compounds, displaying regions of axial, conical, and planar magnetic structures (●, transition temperatures obtained from ac susceptibility measurements; ○, obtained from cone-angle measurements). The shaded vertical boundary is tentative, and marks the separation between the cone-2 and the planar regions.

$$\chi_H \approx |t|^{-\omega_{\text{SR}}}, \quad (7a)$$

and therefore χ_H should show scaling behavior. Now, for $t > 0$ ($T > T_{\text{SR1}}$), indeed $\beta_{\text{SR}} = 0$ and therefore $\omega_{\text{SR}} = \gamma_{\text{SR}}$ and

$$\chi_H \approx t^{-\gamma_{\text{SR}}}. \quad (7b)$$

(ii) We will consider now the alternative approach $H \rightarrow 0$ (for the critical isotherm $t = 0$), and therefore we will have

$$\theta \approx H^{1/\delta_{\text{SR}}} g(t/H^{1/\beta_{\text{SR}}\delta_{\text{SR}}}). \quad (8)$$

For $t = 0$, from (4) and (8) one immediately obtains that

$$\chi_H = \frac{1}{\delta_{\text{SR}}} M_S H^{2/\delta_{\text{SR}}-1} [g(x)]^2, \quad (9)$$

from which, considering that $g(x) = \text{const}$ for $x = 0$,

$$\chi_H \approx H^{2/\delta_{\text{SR}}-1}. \quad (10)$$

Notice that for both paths, the angular susceptibility χ_θ behaves as

$$t \rightarrow 0, \quad \chi_\theta \approx |t|^{-\gamma_{\text{SR}}}, \quad (11a)$$

$$H \rightarrow 0, \quad \chi_\theta \approx H^{1/\delta_{\text{SR}}-1}, \quad (11b)$$

indeed in the same way as χ_H for an ordinary paraferromagnetic phase transition, where M_S is the order parameter.

On the other hand, when \mathbf{M}_S approaches the transition reorientation angle $\theta_f \equiv \theta(T_{\text{SR2}})$ for $T \gtrsim T_{\text{SR2}}$ [which is the case for the $(\text{Er}_x\text{Nd}_{1-x})_2\text{Fe}_{14}\text{B}$ compounds for $0.2 \leq x \leq 0.6$], the order parameter now to be taken is the deviation angle of \mathbf{M}_S from the orientation θ_f , i.e.,

$\phi = \theta_f - \theta$. Now the scaling that applies for $T > T_{\text{SR2}}$ should be,

$$\phi = |t|^{\beta_{\text{SR2}}} f(H/|t|^{\beta_{\text{SR2}}\delta_{\text{SR2}}}), \quad (12)$$

where $t = (T - T_{\text{SR2}})/T_{\text{SR2}}$. A calculation very similar to the previous one for $T < T_{\text{SR1}}$ gives a more complex result for $T > T_{\text{SR2}}$:

$$t \rightarrow 0, \quad \chi_H \approx |t|^{-\gamma_{\text{SR2}}} (k_1 + k_2 |t|^{\beta_{\text{SR2}}} + k_3 |t|^{2\beta_{\text{SR2}}}) \quad (H=0), \quad (13a)$$

$$H \rightarrow 0, \quad \chi_H \approx H^{1/\delta_{\text{SR2}}-1} (k'_1 + k'_2 H^{1/\delta_{\text{SR2}}} + k'_3 H^{2/\delta_{\text{SR2}}}) \quad (t=0), \quad (13b)$$

where k_1, \dots and k'_1, \dots are arbitrary constants, and where the critical exponents are, in principle, different from the ones at T_{SR1} . Since the term $t^{-\gamma_{\text{SR2}}}$ in (13a) [or $H^{1/\delta_{\text{SR2}}-1}$ in (13b)] gives a divergence at $t = 0$ [or $H = 0$ if $(1/\delta_{\text{SR2}} - 1) < 0$], then the contributions $t^{\beta_{\text{SR2}}}, t^{2\beta_{\text{SR2}}}$ (or $H^{1/\delta_{\text{SR2}}}, H^{2/\delta_{\text{SR2}}}$) in Eqs. (13) are probably not important, as they are for $\theta = 0$. On the other hand, for $T < T_{\text{SR2}}$, θ should be either essentially constant or increasing towards its final value at $T = 0$, i.e., $\theta = \theta(T_{\text{SR2}}) + \phi$. This is actually the case for the $(\text{Er}_x\text{Nd}_{1-x})_2\text{Fe}_{14}\text{B}$ compounds for $x = 0.2, 0.4$ [Fig. 2(b)]. This situation is not actually manifested in Fig. 2, due to the experimental error in the SR angles measured by the polar plot method.¹⁰ However, measurements of the SR angle obtained by the measurement of the magnetization components parallel and perpendicular to the tetragonal c axis (using magnetically aligned powder samples¹⁰) do show the above-mentioned increase. The total variations of ϕ were of $\approx 1.5^\circ$ and $\approx 0.5^\circ$ for $x = 0.2$ and 0.4 , respectively [see Fig. 2(b) insets]. Now the scaling adopts the form of Eqs. (13) as well, but with the critical exponent γ'_{SR2} and different constants k_i and k'_i indeed.

III. RESULTS AND DISCUSSION

The preceding ideas arose as a consequence of the measurements of the initial ac susceptibility and coning angles¹⁰ in the above-mentioned pseudoternaries $(\text{Er}_x\text{R}_{1-x})_2\text{Fe}_{14}\text{B}$ ($R = \text{Nd}$ and Dy), with competitive anisotropies, and therefore undergoing magnetic SR phase transitions. The susceptibility was measured between 3.5 and ≈ 350 K using a commercial mutual inductance bridge, working at 15 Hz and with ac magnetic fields in the primary coils of around 30 mOe peak values typically. The SR cone angles were determined by measuring the magnetization component perpendicular, M_\perp , to the applied magnetic field when this is within a plane which contains the tetragonal c axis.¹⁶ In fact, when the turning field coincides with the easy magnetization axis, $M_\perp = 0$ and this method allows us to determine θ . The samples were in the form of powders ($\approx 50 \mu\text{m}$ average grain size) aligned by a strong magnetic field ($\approx 2.5T$) within a fixing epoxy resin and shaped to disks.

The present pseudoternaries were prepared by arc melting from stoichiometric amounts of R (99.9% puri-

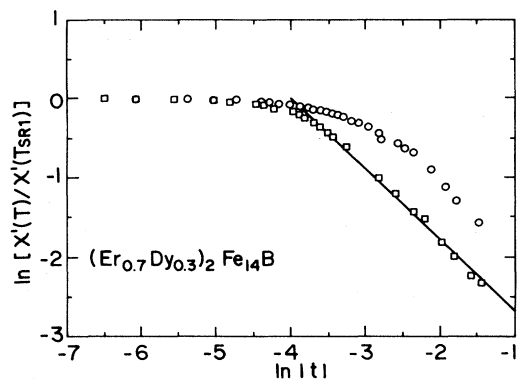


FIG. 4. Double logarithmic scaling of the initial susceptibility, χ' , for the $(\text{Er}_{0.7}\text{Dy}_{0.3})_2\text{Fe}_{14}\text{B}$ system, above (\square) and below (\circ) the SR transition temperature $T_{\text{SR1}} = 129.7$ K. In the vertical axis is the reduced susceptibility $\chi'(T)/\chi'(T_{\text{SR1}})$ and in the abscissa the absolute reduced temperature $|t| \equiv |T - T_{\text{SR1}}|/T_{\text{SR1}}$. The straight line is the least-squares fit in the region where critical scaling is supposed to apply. The obtained critical exponent from the slope of the line is $\gamma_{\text{SR}} = 0.89 \pm 0.05$.

ty), Fe (99.99%), and Boron. The buttons obtained were annealed at 950°C during around 110 hours, and x-ray analyzed by the Debye-Scherrer powder method. The measured lattice constants were in good agreement with published data^{15,17} and no secondary phases were detected by this method (5% confidence).

In Fig. 1(a) we can see the thermal variation of χ' for the $(\text{Er}_x\text{Dy}_{1-x})_2\text{Fe}_{14}\text{B}$ series and we can observe strong anomalies (for $x \geq 0.6$) that we have associated with the SR transitions, at T_{SR1} (Ref. 9). Such anomalies are clearly superposed to a background of susceptibility, which decreases with temperature as expected from the usual Hopkinson effect, i.e., the pinning by anisotropy forces of the narrow domain walls observed¹⁸ in materials

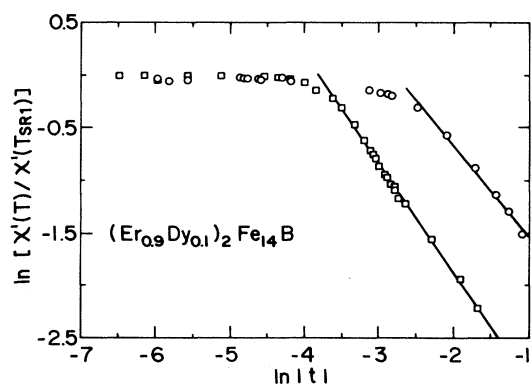


FIG. 5. The same as for Fig. 4 for the $(\text{Er}_{0.9}\text{Dy}_{0.1})_2\text{Fe}_{14}\text{B}$ system ($T_{\text{SR1}} = 267.1$ K). The critical exponents obtained from the lines slopes are $\gamma_{\text{SR}} = 1.03 \pm 0.05$ (for the critical regime above T_{SR1} , \square) and $\omega'_{\text{SR}} = 0.85 \pm 0.05$ (for the critical regime below T_{SR1} , \circ).

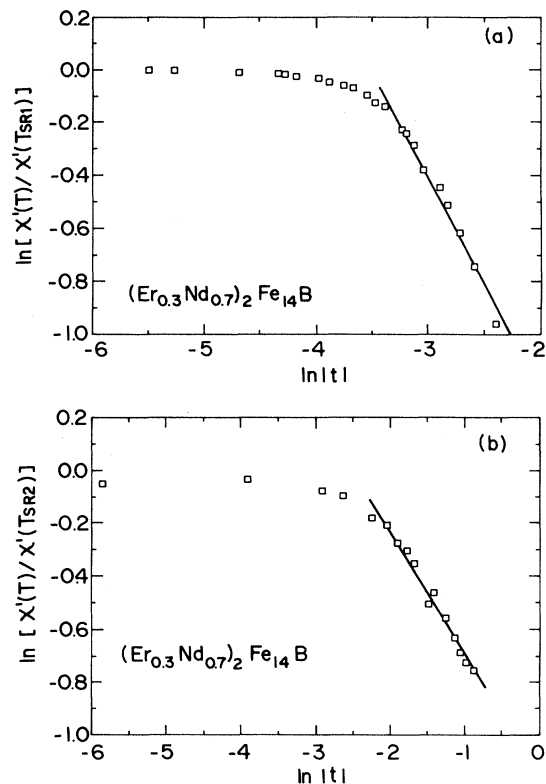


FIG. 6. (a) Double logarithmic scaling of the initial susceptibility, χ' , for the $(\text{Er}_{0.3}\text{Nd}_{0.7})_2\text{Fe}_{14}\text{B}$ system above the first reorientation transition temperature $T_{\text{SR1}} (=137.7$ K). In the vertical axis is the reduced susceptibility $\chi'(T)/\chi'(T_{\text{SR1}})$ and in the abscissa the absolute reduced temperature $|t| \equiv |T - T_{\text{SR1}}|/T_{\text{SR1}}$. The straight line is the least-squares fit in the region where critical scaling is supposed to apply. The deduced critical exponent from the slope of the line is $\gamma_{\text{SR1}} = 0.79 \pm 0.05$. (b) The same as for (a), for the second SR transition at temperature $T_{\text{SR2}} = 17.5$ K. The obtained critical exponent above T_{SR2} is $\gamma_{\text{SR2}} = 0.45 \pm 0.05$.

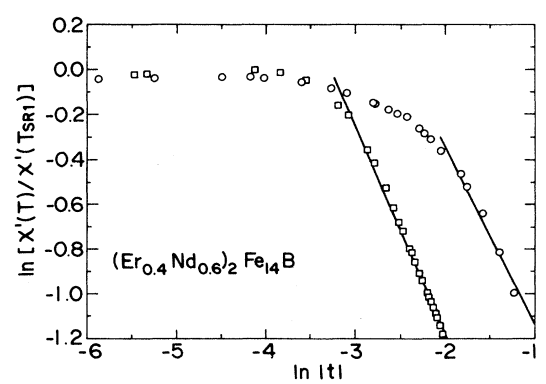


FIG. 7. The same as for Fig. 6(a) for the $(\text{Er}_{0.4}\text{Nd}_{0.6})_2\text{Fe}_{14}\text{B}$ system above (\square) and below (\circ) the first SR transition at $T_{\text{SR1}} = 142.5$ K. The resulting critical exponents are $\gamma_{\text{SR1}} = 0.92 \pm 0.05$ (above T_{SR1}) and $\omega'_{\text{SR1}} = 0.78 \pm 0.05$ (below T_{SR1}).

of so large an anisotropy, where the walls have low mobility as well. Therefore, in order to perform a sensible scaling of χ' we have subtracted, at the critical region, the anomalies from the background, this obtained from a suitable extrapolation of $\chi'(T)$ at both sides of the anomalous region. As we can observe, the increase in Dy content depresses T_{SR1} , in good agreement with CEF calculations.¹¹

In order to extract the critical exponents, we have proceeded to scale χ' versus t using double logarithmic plots and some typical results are displayed in Figs. 4 and 5, for both branches $t > 0$ and $t < 0$. As we may observe, scaling is rounded off for T relatively far from T_{SR1} , where the plots become completely flat. It is therefore important to recognize that the extraction of the critical exponents γ_{SR} and ω'_{SR} in the present kind of transition is quite hard, inasmuch as (see Figs. 4–10) a good deal of the critical region is covered by demagnetizing field (strong for a ferromagnet, which happens to be the case here) and rounding effects. The flattening effect near T_{SR} can be explained as follows. For a finite sample the measured apparent susceptibility, χ'_{ap} , is related to the true one, χ'_t , by

$$\chi'_{ap} = \frac{1}{(1/\chi'_t) + N}. \quad (14)$$

Therefore, if χ'_t diverges at $T \rightarrow T_{SR1}$, $\chi'_{ap} \rightarrow 1/N$ and becomes constant as observed in Figs. 4–10 (the samples were in the form of prisms of $\approx 12 \times 1 \times 1$ mm³). Moreover, rounding effects due to sample inhomogeneities¹⁹ and critical slowing down of the SR relaxation times beyond the time period (66 msec) of the measuring ac field cannot be ruled out. Now, in order to extract the critical exponents [see Eqs. (7a) and (7b)] we have considered the slope of the portions nearest to the flat ones (in order to be as near to T_{SR1} as feasible), which are distinctively linear. The rounded portions connecting such regions are quite a problem for the determination of the critical region below T_{SR1} and T_{SR2} and throw some uncertainty on the determination of the critical exponents ω'_{SR} and γ'_{SR} . But for the critical regimes above the tran-

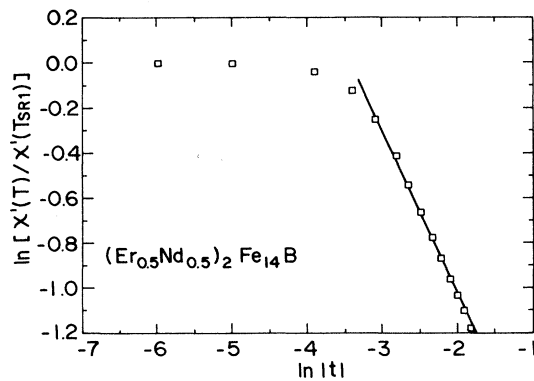


FIG. 8. The same as for Fig. 6(a) for the $(\text{Er}_{0.5}\text{Nd}_{0.5})_2\text{Fe}_{14}\text{B}$ system. The critical exponent, above $T_{SR1} = 150.5$ K, becomes $\gamma_{SR1} = 0.71 \pm 0.05$.

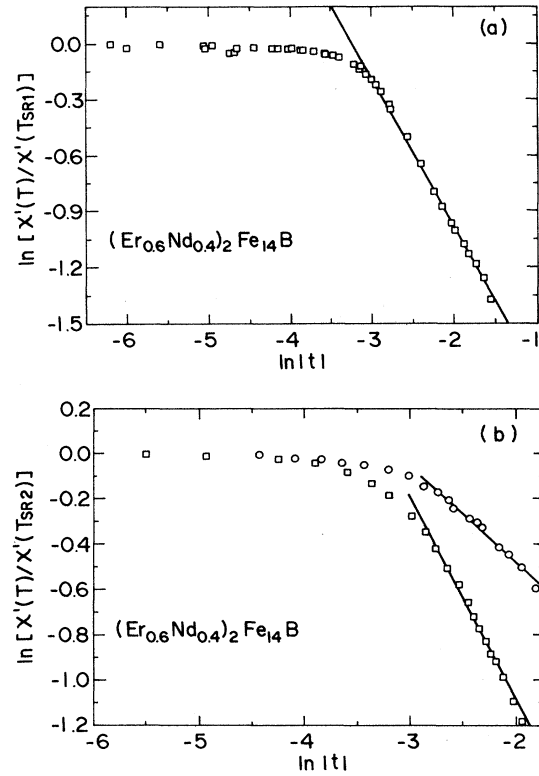


FIG. 9. (a) The same as for Fig. 6(a) for the $(\text{Er}_{0.6}\text{Nd}_{0.4})_2\text{Fe}_{14}\text{B}$ system. The critical exponent, above $T_{SR1} = 162.7$ K, becomes $\gamma_{SR1} = 0.79 \pm 0.05$. (b) The same as for Fig. 7 for the $(\text{Er}_{0.6}\text{Nd}_{0.4})_2\text{Fe}_{14}\text{B}$ system. The critical exponents become $\gamma_{SR2} = 0.88 \pm 0.05$ (above $T_{SR2} = 42.0$ K, \square) and $\gamma'_{SR2} = 0.42 \pm 0.05$ (below T_{SR2} , \circ).

sition temperatures the double log plots show large linear portions, the critical exponents so determined being quite confident. Nevertheless, we have discarded those compounds and transitions where the obtention of the critical exponents was not quite trustworthy. The values of the exponents $\omega'_{SR} \equiv \gamma'_{SR} - \beta_{SR}$ and γ_{SR} obtained are shown in

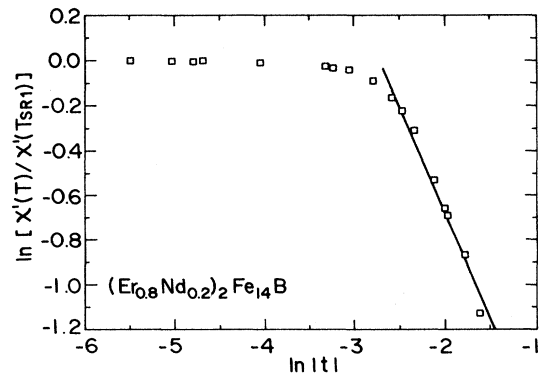


FIG. 10. The same as for Fig. 6(a) for the $(\text{Er}_{0.8}\text{Nd}_{0.2})_2\text{Fe}_{14}\text{B}$ system. The critical exponent becomes $\gamma_{SR1} = 0.93 \pm 0.05$, above $T_{SR1} = 206.7$ K.

the captions of Figs. 4 and 5 for different compounds of the $(\text{Er}_x\text{Dy}_{1-x})_2\text{Fe}_{14}\text{B}$ series.

Similarly, in Figs. 1(b)–1(d) we show the results of the measurement of χ' for the $(\text{Er}_x\text{Nd}_{1-x})_2\text{Fe}_{14}\text{B}$ series. As we can see for $0.2 \leq x \leq 0.6$ there appear two peak anomalies, which we associate with the temperatures T_{SR1} and T_{SR2} discussed before.⁹ We have proceeded as well to perform a scaling analysis at both anomalous regions, in order to extract ω'_{SR1} and γ'_{SR1} from the first transition as before, and γ'_{SR2} and γ'_{SR2} from the second one [see Eq. (13a)], and the performed scalings are shown in Figs. 6–10. The critical exponents are shown in the

captions of these figures, and the same comments and restrictions as for the Dy substituted compounds are pertinent now.

Measurements of the field dependence of χ' at the critical isotherms, as well as a detailed study of the field and temperature dependence of the coning angles near the SR transition temperatures, are in progress.

ACKNOWLEDGMENTS

We are grateful to the Spanish CICYT for financial support under Grant No. MAT88-0552 and to the CEAM Programme II of the European Communities.

-
- ¹See, for instance, K. P. Belov, A. K. Zvezdin, A. M. Kadomseva, and R. Z. Levitin, *Usp. Fiz. Nauk.* **119**, 447 (1976) [*Sov. Phys. Usp.* **19**, 574 (1976)] and references therein; also M. B. Salamon and D. S. Simons, *Phys. Rev. B* **7**, 229 (1973).
- ²E. Tatsumoto, T. Okamoto, H. Fujii, and C. Inoue, *J. Phys. (Paris)* **32**, 550 (1971).
- ³A. del Moral, P. A. Algarabel, and M. R. Ibarra, *J. Magn. Magn. Mater.* **69**, 285 (1987), and references therein.
- ⁴M. R. Ibarra, O. Moze, P. A. Algarabel, J. I. Arnaudas, J. S. Abell, and A. del Moral, *J. Phys. C* **21**, 2735 (1988); paper related to SR transition in HoAl_2 .
- ⁵P. A. Algarabel, A. del Moral, M. R. Ibarra, and J. I. Arnaudas, *J. Phys. Chem. Solids* **49**, 213 (1988); paper related to SR transitions in hexagonal hard intermetallics.
- ⁶See, for instance, *Nd-Fe Permanent Magnets*, edited by I. V. Mitchell (Elsevier, London, 1985).
- ⁷J. M. D. Coey, *J. Less-Common Met.* **126**, 21 (1986).
- ⁸H. R. Rechenberg, J. P. Sanchez, P. L'Héritier, and R. Fruchart, *Phys. Rev. B* **36**, 1865 (1987).
- ⁹M. R. Ibarra, C. Marquina, P. A. Algarabel, J. I. Arnaudas, and A. del Moral, *Solid State Commun.* **69**, 131 (1989).
- ¹⁰M. R. Ibarra, C. Marquina, P. A. Algarabel, J. I. Arnaudas, and A. del Moral, *J. Appl. Phys.* **64**, 5537 (1989).
- ¹¹M. R. Ibarra, P. A. Algarabel, C. Marquina, J. I. Arnaudas, A. del Moral, L. Pareti, O. Moze, G. Marusi, and M. Solzi, *Phys. Rev. B* **39**, 7081 (1989).
- ¹²P. A. Algarabel, M. R. Ibarra, C. Marquina, G. Marusi, O. Moze, L. Pareti, M. Solzi, J. I. Arnaudas, and A. del Moral, *Physica B* **155**, 263 (1989).
- ¹³D. Givord, H. S. Li, and R. Perrier de la Bâthie, *Solid State Commun.* **55**, 857 (1984).
- ¹⁴A. Hankey and H. Stanley, *Phys. Rev. B* **6**, 3515 (1972).
- ¹⁵S. Sinnema, R. Y. Radwanski, J. J. M. Franse, D. B. de Mooij, and K. H. J. Buschow, *J. Magn. Magn. Mater.* **44**, 33 (1984).
- ¹⁶E. Joven, A. del Moral, and J. I. Arnaudas (unpublished); A. del Moral, E. Joven, M. R. Ibarra, J. I. Arnaudas, J. S. Abell, and P. A. Algarabel, *J. Phys. (Paris) Colloq.* **12**, C8-449 (1988).
- ¹⁷S. Hirosawa, Y. Matsuura, H. Yamamoto, S. Fujimura, and M. Sagawa, *J. Appl. Phys.* **59**, 873 (1986).
- ¹⁸W. D. Corner and M. J. Hawton, *J. Magn. Magn. Mater.* **72**, 59 (1988).
- ¹⁹Measurements of magnetic anisotropy using the SPD (singular point detection technique) in fact show the presence of small amounts of a secondary phase, not identified.